Progress in Organic Coatings

ORGANIC COATINGS
An International Journal

Three-dimensional analysis of the spatial distribution of iron oxide particles in a decorative coating by electron microscopic imaging

CrossMark

Bo Chen [a,e,*], Teruo Hashimoto [b], Frank Vergeer [c], Andrew Burgess [d], George Thompson [b], Ian Robinson [a,e,*]

[a] London Centre for Nanotechnology, University College London, WC1H 0AH, UK
[b] Corrosion & Protection Centre, School of Materials, The University of Manchester, Manchester M13 9PL, UK
[c] AkzoNobel Co. Ltd., Sassenheim 2171AJ, The Netherlands
[d] AkzoNobel (UK) Co. Ltd., Felling, Gateshead, Tyne and Wear NE10 0JY, UK
[e] Research Complex at Harwell, Harwell Oxford, Didcot, Oxfordshire OX11 0FA, UK

ARTICLE INFO

ABSTRACT

The three-dimensional (3D) spatial structure of an iron oxide containing alkyd paint specimen has been investigated by serial block-face scanning electron microscopy (SBFSEM). The resultant images of the 3D structure clearly present the spatial distribution of the iron oxide pigment particles in the coating film and reveal the extent of aggregation of the particles in the matrix material. More than one-half of the iron oxide particles (in volume) had aggregated to form clusters of considerable sizes that follow a Gaussian spacing distribution in the measured coating film. Over 80% of the clusters have dimensions between 1.5 μm and 3.5 μm; also, pores are evident at the centres of clusters whose sizes are larger than 2 μm. The work demonstrated here reveals a new approach to fully characterize the 3D spatial structure of coatings and to explore their correlations with the performance of the materials.

1. Introduction

The spatial distribution of pigment particles in the matrix material of coatings [1] is a main concern for the coating industry since it determines the visual appearance and it affects the performance of the cured coating films [2]. With regard to pigments, their incorporation can strengthen the coating or produce some specific properties such as ultraviolet (UV) resistance [2,3], self-cleaning [4], anti-corrosive [5] and anti-fouling [6] capabilities of the coating. The previous properties are heavily influenced by the pigment distribution in the cured films. In this study, we have revealed the detailed 3D structure of an alkyd resin based decorative paint to present the spatial distribution of the iron oxide pigment particles within the coating. The selected paint represents one of the most widely used and most important types of coating since the 1930s after the synthesis of alkyd resin [7–9]. The structure of this type of coating has been investigated previously by X-ray [10] and electron [11] probes in two-dimensions. Here, serial

block-face scanning electron microscopy (SBFSEM) [1,12,13], a 3D electron imaging method combined with a serial-sectioning technique [14,15], which is widely used for biological sample structure visualization [16–18], was employed to fulfil the objective of 3D structure investigation of the paint.

The measured alkyd paint mainly comprises iron oxide particles and alkyd resin, which are the pigment and matrix material of the coating respectively. The specimen is a piece of cured coating which was prepared by mixing in a Skandex BA-S mixer (serial number 320-209-3882, from Harbil International B.V.) shaking machine for 3 min, the same mixing time as usually applied on the job-site, before being applied to a polypropylene (PP) plate by a K-control coater. The coating film was cured at room temperature for one month after the application, and then stored in a sealed light tight paper envelope for one and half years before the measurement. This type of iron oxide containing alkyd resin based decorative coating could produce high level UV resistant capabilities, which are determined by the spatial distribution of the iron oxide particles within the coating film. The extent of the iron oxide particle dispersion in the matrix resin is critical for producing coatings with efficient UV resistant performance, long service life and precise colour. Additionally, the cost of a decorative paint is dominated by the amount of pigments used since they are the most expensive component in the coating material. An optimized dispersion of the pigments, here

* London Centre for Nanotechnology, University College London, 17-19 Gordon Street, London, WC1H 0AH, UK. Tel.: +44 2076799929.
E-mail addresses: chenwillcon@gmail.com (B. Chen), i.robinson@ucl.ac.uk (I. Robinson).

the iron oxide particles, will lead to minimizing the amount of pigment used. Further, this is the preferred way to reduce the cost of the coatings. Revealing the 3D structure of the coating is the only way to fully observe the true spatial distribution of these pigment particles and to explore the correlations between the 3D structure and the performance of the coating.

2. Experiment

Different from X-ray computed tomography [19,20], SBFSEM obtains 3D images by acquiring successive parallel images of fresh surfaces of the samples produced by iterative slicing with a diamond knife driven by an ultramicrotome system installed in the scanning electron microscope chamber [1,12]. Samples for the SBF-SEM measurement have to be fixed first. The fixations are usually achieved by embedding the samples into epoxy resin blocks [17,21]. However, since the sample here is a piece of a cured, free-standing thin coating film, about 25 μm thick, which was peeled from the substrate, it was fixed by glueing it directly on to a flat aluminium specimen slide using cyanoacrylate glue rather than embedding in epoxy resin. Once the glue had cured, the specimen and its supporting aluminium slide were trimmed using an external, conventional ultramicrotome to create a block face of dimensions of around 500 μm × 500 μm at the tip of the specimen. Subsequently, the trimmed sample was mounted in the GATAN 3View sample holder, and then it was measured by the SBFSEM system which was installed in a field emission gun (FEG) environmental SEM from FEI (QUANTA 250 FEGESEM). The system was operated at 2.5 kV with 70 Pa chamber pressure in a water vapour environment. The back scattering electron (BSE) signals from the sample were acquired by the detector with an output image pixel size of 15 nm × 15 nm. The nominal sectioning thickness was 15 nm per slice. The sample surface, attached to the aluminium slide by the glue, was placed perpendicular to the moving direction of the diamond knife. Consequently, cross-sections of the coating film from the surface to the coating-substrate interface were imaged during measurement. Overall, 1000 slice images (producing a 15 μm thick stack) with a field of view 30.7 μm × 30.7 μm were obtained after about 8 h serial sectioning and electron beam imaging.

3. Results and discussion

Fig. 1 demonstrates the results of SBFSEM probing of the alkyd paint sample. As the specimen mainly consists of two components, according to the BSE imaging mechanism, in Fig. 1a and b, the bright features are iron oxide particles, and the remaining regions (between the surface and interface in Fig. 1a) are alkyd resin. The bright line indicated by the yellow arrow at the left of Fig. 1a is the cyanoacrylate glue. It was used to fix the sample, and was rendered as a transparent white layer in Fig. 1c. As shown in three dimensions in Fig. 1c, the spatial distribution of free iron oxide particles and the clusters in a whole piece of cured coating film that extends from the surface to the interface are readily revealed. Clearly, there is a considerable amount of clustering of iron oxide particles in the material, which would hinder the coating film from providing optimized performance.

It is evident that the SEM serial sectioning approach has sufficient resolution to reveal isolated, individual pigment particles within the enveloping matrix materials. We can see from Fig. 1, both in 2D and 3D, that the shape of the iron oxide particles is not spherical, but ellipsoidally shaped with aspect ratios around 2 (see Fig. 2b). Here, the aspect ratio, AR, of a particle is defined as the ratio of its length to width. The length and the width of an object are the maximum and the minimum of the Feret diameters [22] of the object respectively. They are obtained from Avizo after 3D

Table 1
Statistics of volumes of different fractions in the measured sample.

Fractions	Volume/μm^3	Volume concentration/%
Intact clusters[a]	106.12	1.11
Incomplete clusters[a]	8.50	0.09
Remaining iron oxide particles	97.56	1.02
Alkyd resin	9314.65	97.77

[a] Here, the clusters mean the clusters of iron oxide particles.

image segmentation. The sizes (in length) of the majority of particles, over 75%, lie between 100 nm to 500 nm (see Fig. 2a). This is in good agreement with the information provided by the manufacturer that the maximum size of the iron oxide pigment particles is 500 nm. The statistical result of widths, lengths and volumes of all the resolved particles smaller than 500 nm (in width), based on the segmentation of the 3D image, is listed in Supplementary Table S1. From this, it is clear that the average size (in length) and the volume of individual iron oxide particles are 370 nm and 7.47×10^{-3} μm^3 respectively.

Supplementary Table S1 related to this article can be found, in the online version, at http://dx.doi.org/10.1016/j.porgcoat.2014.03.005.

As shown in Figs. 1c and 3a, a large number of iron oxide particles have agglomerated together to form clusters in the coating film after the treatment. The majority of clusters are also ellipsoidally shaped with aspect ratios around 1.8 (see Figs. 3 and 4b) and pores were located in the centre regions of the larger clusters (see Figs. 1b and 3b & c); such clusters are normally larger than 2 μm. The formation of pores in the clusters may be caused by the magnetic force of iron oxide particles which stops them stacking together and growing into large solid clusters, and drives the particles to cluster into a hollow ring shape to balance the external magnetic forces among themselves. Based on the segmentation of the obtained 3D structure, the volume concentration (VC) of iron oxide pigment is 2.23%, the sum of the VCs of the first 3 items listed in Table 1, which agrees well with the expected VC of iron oxide pigment provided by manufacturer: 2.0%. There is a large fraction of volume, over 50%, of the particles formed into clusters of considerable sizes, which indicates the current treatment, 3 min mixing in a shaking machine, left a high probability for the iron oxide particles to cluster. Compared with a coating with a homogenous distribution of the pigment, this would reduce both capabilities of the coating to scatter visible light and to absorb UV light, and increase the real cost of manufacturing.

The sizes of clusters (in length) range from 1.0 to 6.5 μm as displayed in Fig. 4a and are numerically presented in Supplementary Table S2. These iron oxide particle clusters have a relatively narrow size distribution, with 80% of them being between 1.5 and 3.5 μm. The reason of this is unclear; it may be caused by the diffusion limits. From the statistical figures in Supplementary Table S2, the average length and volume of the clusters are 2.5 μm and 1.9 μm^3 respectively. The scattering capability of a cluster of this size would be much less than the total scattering capabilities of 254 free iron oxide particles, which is the average number of free particles in one cluster (obtained by dividing the average volume of a cluster, 1.9 μm^3, by the average volume of a free iron oxide particle, 7.47×10^{-3} μm^3). This would act to degrade the colour and covering power of the coating. The UV resistance capability of the coating would decrease as well because of the reduction of the total surface area of iron oxide particles. In order to improve the performance of the coating, the dispersion of the iron oxide particles needs to be enhanced by using ways such as extending the mixing time of the coating material before application. However, no settlement occurred during the curing process and
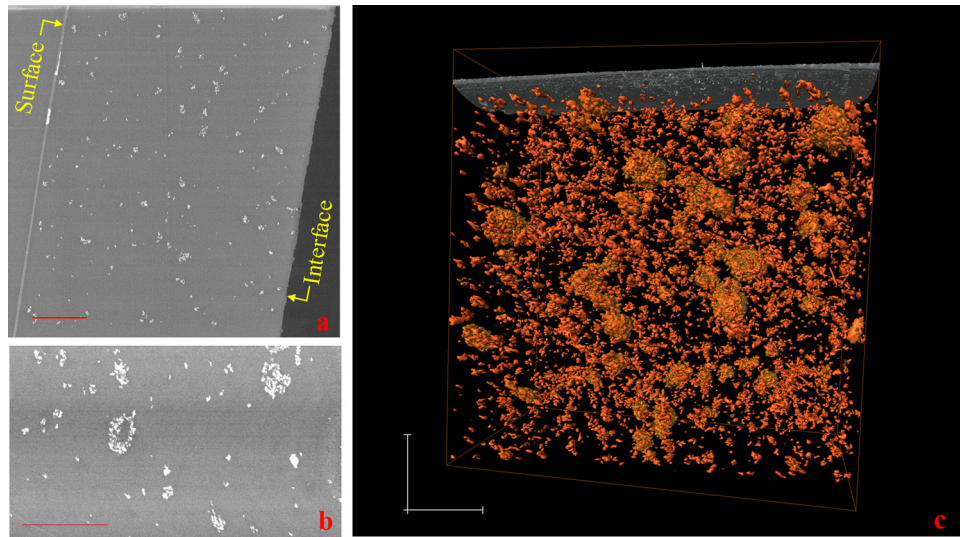
Fig. 1. Results for the alkyd paint sample by SBFSEM measurements: (a) an (original) SBFSEM section slice showing the glue covered "surface" and peeled-off "interface"; (b) a slice-cut parallel to the sample surface; (c) rendering of the acquired 3D volume of the sample. The transparent white layer on the top is the cyanoacrylate glue contacted with the sample surface, the orange parts are iron oxide particles, and the clusters were rendered with transparent yellow surface. The 3D image segmentation and rendering were carried out by Avizo. The scale bars are 5 μm.
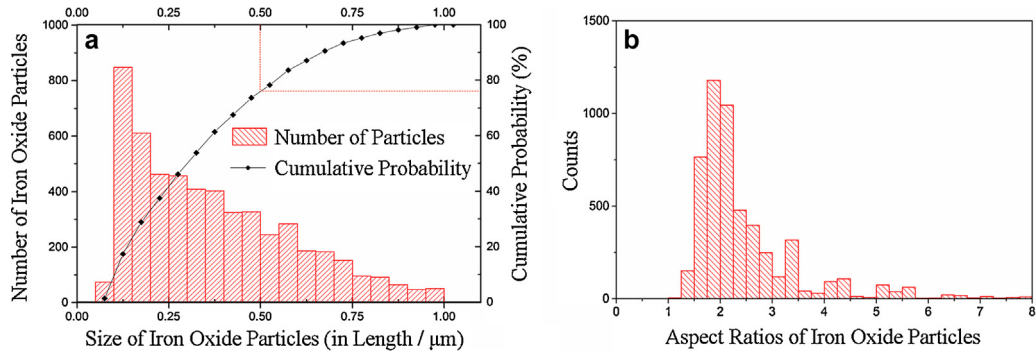

Fig. 2. Characterization of the iron oxide particles: (a) a histogram (with 0.05 μm step) of size distribution of the iron oxide particles with the curve of cumulative probability and (b) a histogram (with step of 0.25) of aspect ratios of the iron oxide particles.
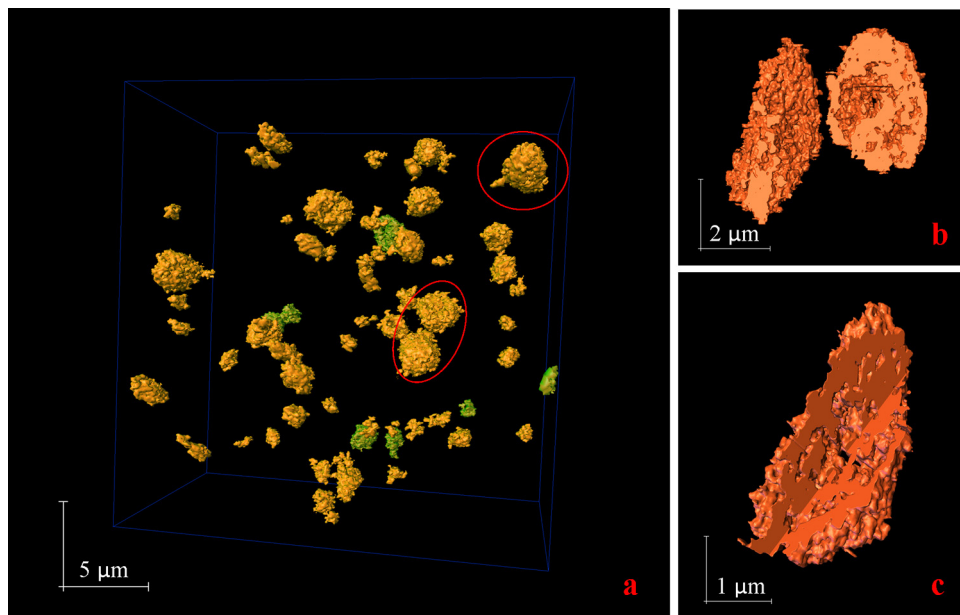

Fig. 3. 3D rendering of the clusters of iron oxide particles: (a) distribution of the clusters of iron oxide particles within the coating film. The non-clustered particles have been suppressed for clarity. All the intact clusters are in yellow and the incomplete ones are covered by green; (b) 3D rendering of two of the clusters circled by a red ellipse in panel a. The cut-through of the right one was shown; and (c) 3D rendering of one of the clusters circled by a red ellipse at the top-right corner in panel a. The cut-through from two different orientations was shown. (For interpretation of the references to color in this legend, the reader is referred to the web version of the article.)
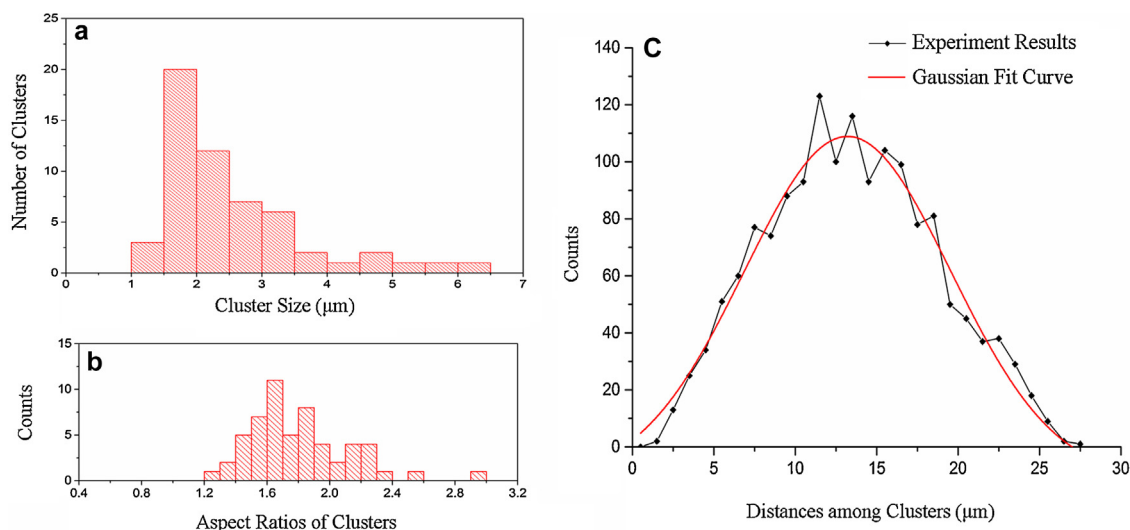
Fig. 4. Characterization of 3D spatial distribution of the clusters of the iron oxide particles: (a) a histogram (with 0.5 μm step) of size distribution of the intact clusters of the iron oxide particles; (b) a histogram (with step of 0.1) of aspect ratios of the clusters of the iron oxide particles; (c) a histogram (with 1 μm step and in black dot-line) of distribution of distances among individual clusters with Gaussian fit result (in red line). (For interpretation of the references to color in this legend, the reader is referred to the web version of the article.)

the clusters are dispersed all over the material as demonstrated in Figs. 1c and 3a. From Fig. 4c, we further see that the distribution of distances among individual clusters follows a Gaussian law, $f_{(x)} = 120.02e^{-((x-13.21)^2)/80.52} - 11.25$, with a mean distance of about 13 μm. Even though the distribution is cut off by the size of the measured sample volume, this suggests that the spacing among the clusters is determined by diffusion process of the iron oxide particles in the alkyd resin.

Supplementary Table S2 related to this article can be found, in the online version, at http://dx.doi.org/10.1016/j.porgcoat.2014.03.005.

4. Conclusions

SBFSEM has been shown to be an effective method to investigate the 3D structure of condensed materials. The system provides electron microscopy resolution in the imaging planes, which enables resolution of nano-scale targets with imaging of a relatively large volume. However, it is a destructive method because the diamond knife has direct physical contact with the imaging surfaces, which could potentially lead to deformation of shapes and movement of positions of features in the specimens, for example the iron oxide particles in this study.

The 3D spatial structure of the iron oxide containing alkyd paint was revealed and was quantitatively analyzed. Over one-half of the iron oxide particles (in volume) formed into clusters of considerable sizes, which indicates that the mixing methodology employed did not produce a coating with homogenously dispersed pigment after curing. Ways, such as extending the mixing time or optimizing the dispersing agent, should be employed to improve the pigment dispersion in the matrix material. The clusters of iron oxide particles are ellipsoidally shaped and follow a Gaussian spacing distribution in the measured coating sample. They have a preferred size range between 1.5 μm and 3.5 μm, with pores in the centres of clusters that are probably larger than 2 microns. The clustering reduces the total surface area of iron oxide particles in the coating, which acts to reduce both visible light scattering and the UV light absorbing capabilities of the cured film, and to degrade its appearance and performance.

The results will help to understand the real shapes, sizes and dispersion of the pigment particles in the coating materials in three dimensions. It will also help to establish the relationship between 3D spatial distribution of pigment particles and coating performance, and it will help to explore optimized ways for coating manufacture and applications.

References

[1] B. Chen, et al., Sci. Rep. 3 (2013) 1177.
[2] R. Lambourne, T.A. Strivens, Paint and Surface Coatings – Theory and Practice, 2nd ed., Woodhead Publishing Ltd., Cambridge, England, 1999, pp. 1–18.
[3] P. Katangur, P.K. Patra, S.B. Warner, Polym. Degrad. Stabil. 91 (2006) 2437–2442.
[4] C. Euvananont, C. Junin, K. Inpor, P. Limthongkul, C. Thanachayanont, Ceram. Int. 34 (2008) 1067–1071.
[5] P.A. Sørensen, S. Kiil, K. Dam-Johansen, C.E. Weinell, J. Coat. Technol. Res. 6 (2009) 135–176.
[6] D.M. Yebra, S. Kiil, K. Dam-Johansen, Prog. Org. Coat. 50 (2004) 75–104.
[7] A. Hofland, Prog. Org. Coat. 73 (2012) 274–282.
[8] P. Uschanov, N. Heiskanen, P. Mononen, S.L. Maunu, S. Koskimies, Prog. Org. Coat. 63 (2008) 92–99.
[9] S.T. Warzeska, et al., Prog. Org. Coat. 44 (2002) 243–248.
[10] B. Chen, et al., New J. Phys. 13 (2011) 103022.
[11] A. Kumar, P.K. Vemula, P.M. Ajayan, G. John, Nat. Mater. 7 (2008) 236–241.
[12] W. Denk, H. Horstmann, PLoS Biol. 2 (2004) e329.
[13] B.R. Arenkiel, M.D. Ehlers, Nature 461 (2009) 900–907.
[14] H. Gay, T.F. Anderson, Science 120 (1954) 1071–1073.
[15] F.S. SjÖstrand, J. Ultrastruct. Res. 2 (1958) 122–170.
[16] J. Rouquette, et al., Chromosome Res. 17 (2009) 801–810.
[17] T. Müller-Reichert, J. Mancuso, B. Lich, K. McDonald, Methods Cell Biol. 96 (2010) 331–361.
[18] K.L. Briggman, M. Helmstaedter, W. Denk, Nature 471 (2011) 183–188.
[19] W.V. Glenn Jr., R.J. Johnston, P.E. Morton, S.J. Dwyer, Invest. Radiol. 10 (1975) 403–416.
[20] A.C. Kak, M. Slaney, Principles of Computerized Tomographic Imaging, Society of Industrial and Applied Mathematics, Philadelphia, PA, 2001.
[21] K.L. Briggman, W. Denk, Curr. Opin. Neurobiol. 16 (2006) 562–570.
[22] H.G. Merkus, Particle Size Measurements: Fundamentals, Practice, Quality, Springer, Netherlands, 2009, pp. 15–19.